Smart Rocks and Wireless Communication Systems for Real-Time Monitoring and Mitigation of Bridge Scour
(Progress Report No. 5)

Contract No: RITARS-11-H-MST
(Missouri University of Science and Technology)

Ending Period: September 30, 2012

PI: Genda Chen
Co-PIs: David Pommerenke and Rosa Y. Zheng

Program Manager: Mr. Caesar Singh

Submission Date: October 15, 2012

TABLE OF CONTENTS

EXECUTIVE SUMMARY 1

I - TECHNICAL STATUS.....2

I.1 ACCOMPLISHMENTS BY MILESTONE 2

Task 1.1 Optimal Passive Smart Rock – Engineering design and validation of DC magnetic passive smart rocks ……..... 4

Task 1.2 Steel Interferences to Magnetic Measurements …….……..... 8

Task 2.1 Active Smart Rocks with Embedded Controllable Magnets or with Embedded Electronics …….... 9

Task 2.2(a) Magneto-Inductive Communications – Engineering design and validation of magneto-inductive transponders ……..……..... 12

Task 2.2(b) Acoustic Communications – Engineering evaluation of acoustic communication systems for bridge scour monitoring …….. 12

Task 3.2 Field Validation Planning and Execution ……. 15

I.2 PROBLEMS ENCOUNTERED 15

I.3 FUTURE PLANS 15

II – BUSINESS STATUS 17

II.1 HOURS/EFFORT EXPENDED.....17

II.2 FUNDS EXPENDED AND COST SHARE.....18

EXECUTIVE SUMMARY

In the fifth quarter, the research activities mainly involved the preparation and test of smart rocks at two bridge sites: U.S. Highway 63 – Gasconade River Bridge, Maries County, MO, and Interstate 44 – Roubidoux River Bridge, Pulaski County, MO. The field tests were completed during September 24 – October 3, 2012. Specifically, both passive and active smart rocks were placed in the rivers and tested for their responsiveness, signal strength, and background noise in bridge application environments with the use of a magnetometer and wireless transmission systems. For active smart rocks, both magneto-inductive and acoustic transmission links were tested for their transmission distance, signal fidelity, and power consumption.

Due to limited space, only the test results at the Roubidoux River Bridge were presented for passive smart rocks and the test results at the Gasconade River Bridge for active smart rocks with magneto-inductive wireless transmission. Brief discussion on the acoustic transmission tests at both bridges was included as well.

For field tests, large magnets (2" deep and 4" in diameter) were encased in concrete spheres with a diameter of 10". The concrete spheres were mannually dragged in parallel to a scour-susceptible pier to simulate their potential movement in the process of scour in bridge applications. The encased magnets were demonstrated to be rugged and easy to roll and move at the river beds, which ensure that they will roll to the bottom of a scour hole in application under gravity effects. The data acquired from this series of tests show promise in utilizing rare Earth magnets and a magnetometer as a passive sensing system for bridge scour monitoring. The acquired signals from over 100' away are still strong for easy detection of the presence of magnets. The overall decaying trend of the signals with distance is consistent and repeatable with local fluctuations observed due to potentially changing orientation of the neodymium magnets.

For active smart rocks with magneto-inductive transmission, the peak-peak noise and signal levels are approximately 50 mV and 150 mV, respectively, from a distance of 30'-60'. These results demonstrated a robust operation of wake-up interface via electromagnetic radiation responses from the underwater smart rocks. The maximum communication distance depends on the relative orientation between the smart rock antenna and the receiving antenna bundles. It exceeded 30' from the river bank and 60' from the bridge deck.

The acoustic transmission system also received strong signals from the smart rock located at 3' and 15' away. The communication accuracy was estimated to be a 2% bit error rate. The field testing validated the waterproof casing of smart rock electronic components and acoustic sensors. Additionally, the batteries pack used for active smart rocks continued to supply the required power throughout the testing.

I - TECHNICAL STATUS

I.1 ACCOMPLISHMENTS BY MILESTONE

After the proof-of-concept tests at the Federal Highway Administration's Hydraulics Laboratory in June, 2012, the next step was full scale implementation of both passive and active scour sensor systems (first version of full-scale prototypes). Two bridges in close proximity to Missouri S&T were chosen for full scale testing: Roubidoux Creek Bridge along Interstate 44 in Pulaski County, MO and the Gasconade River Bridge along U.S. Highway 63 in Maries County, MO. The two bridges were chosen out of six due to the river conditions and scour potential of all the bridges available.

Task 1.1 Optimal Passive Smart Rock – Engineering Design and Validation of DC Magnetic Passive Smart Rocks

In the past quarter, large smart rocks were built and prepared for their characterization and validation tests at the two bridge sites. Two types of passive smart rocks were first prepared. The smart rocks were then validated at each bridge site. Following is a brief summary of the field test results and preliminary analysis for I44 – Roubidoux Creek Bridge, Pulaski County, MO.

Design and Casting of Passive Smart Rocks: Two spherical concrete blocks with embedded permanent magnets were cast to present smart rocks. For field tests at bridge sites, each magnet was 4" in diamter and 2" thick. Two passive sensors of various sizes were created. The smaller passive sensor consists of a cylindrical neodymium magnet of dimensions: 2" thick by 4" in diameter. The larger passive sensor consists of two of the afore mentioned magnets placed together to create a larger dipole moment. Normal weight concrete (150 pcf) with a specific gravity of 2.4 was used. The passive sensors themselves have a specific gravity of 7.5. The goal of passive smart rock designs is to encase passive sensors in concrete so that a specific gravity of at least 2.0 can be achieved. To achieve the goal, the only restriction to the passive smart rock design was geometric. Since these magnets are rare earth magnets and very brittle a concrete cover of at least 2" was desired. To consider the same overall dimentions of the two smart rocks, the larger sensor was the limiting factor; it was designed as a shperical concrete block with 10" in diameter as shown in Fig. 1(a). Fig. 1(b) shows the finishing product of two prototype smark rocks for field testing. Figs. 2(a, b) illustrate the casting process of spherical concrete blocks with embedded magnet.

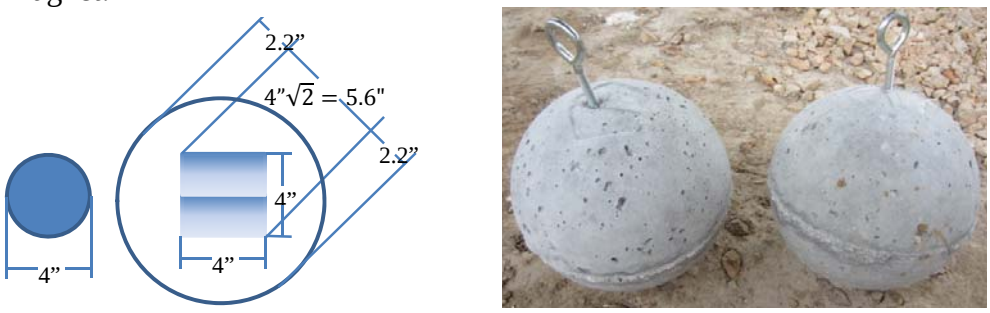

(a) Geometry of magnets and encasement (b) Prototype in spherical shape

Fig. 1 Design and prototype of magnets and passive smart rocks

(a) Bottom half a concrete encasement (b) Top half of a concrete encasement

Fig. 2 Placement of a magnet and casting of spherical concrete block

Test Procedure and Matrices: At the Interstate 44 – Roubidoux Creek Bridge, Pulaski County, MO, two groups of tests were conducted on October 3, 2012, as summarized in 12 test cases in the test matrix in Table 1. One group of tests (all cases except for Case 8 in Table 1) were performed with the magnetometer set at predetermined locations, as illustrated in Fig. 3, while a smart rock was manually dragged in parallel with Pier 7 as shown in Fig. 4 between downstream (north or N) and upstream (south or S). The other group of tests (Case 8 in Table 1) were performed after one smart rock was settled about 4" east of Pier 7 while the magnetometer was moved slowly on the north shoulder of the bridge deck. Each test case in one line orientation of the two magnetometer sensor heads as defined in Table 1 was performed four times to understand the repeatability of test data. For convenience in discussion, a test identification (ID) code (bridge identification:case number:line orientation of two sensor heads) was developed. For example, 44:01:0 represents the test case #1 of I44 bridge with the two magnetometer sensor heads oriented along the river flow direction.

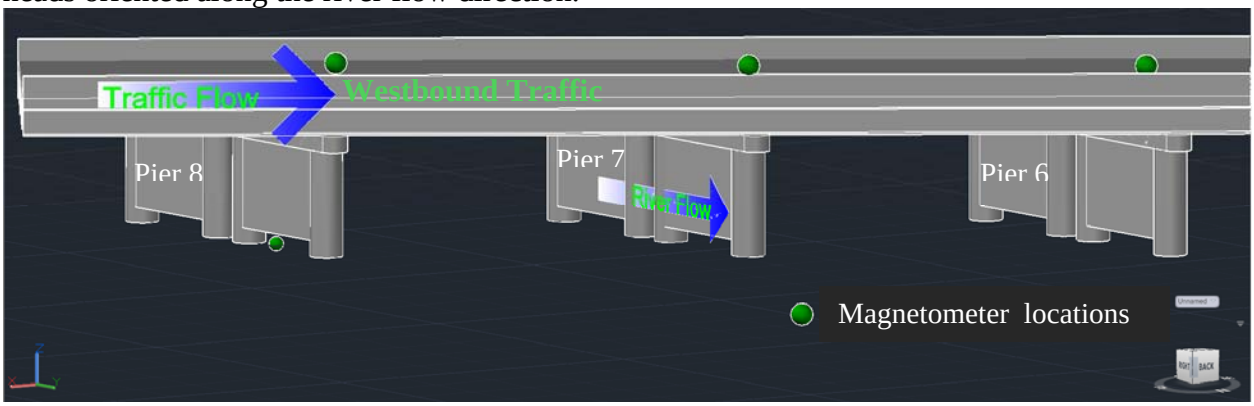

Fig. 3 Interstate 44 – Roubidoux Creek Bridge, Pulaski County, MO test layout

Fig. 4 Movement simulation by manually dragging a prototype smart rock near a bridge pier

Table 1 Test matrix for I44 – Roubidoux Creek Bridge supporting westbound traffic

Case	Magnetometer Location	Sensor Heads Orientation		Magnetomer Movement	Smart Rock Movement	Note
1	Underneath the bridge near Pier 8 (west side)	90		Fixed	N -> S	The weaker smart rock was moved slowly.
		90		Fixed	S -> N	
		90		Fixed	N -> S	
		90	River flow	Fixed	S -> N	
		0		Fixed	N -> S	
		0		Fixed	S -> N	
		0		Fixed	N -> S	
		0	River flow	Fixed	S -> N	
2	On the downstream shoulder of bridge deck at Pier 7	0		Fixed	N -> S	
		0		Fixed	S -> N	
		0		Fixed	N -> S	
		0	River flow	Fixed	S -> N	
3	On the downstream shoulder of bridge deck at Pier 8	0		Fixed	N -> S	
		0		Fixed	S -> N	
		0		Fixed	N -> S	
		0	River flow	Fixed	S -> N	
4	On the downstream shoulder of bridge deck at Pier 6	0		Fixed	N -> S	
		0		Fixed	S -> N	
		0		Fixed	N -> S	
		0	River flow	Fixed	S -> N	
5	On the downstream shoulder of bridge deck at Pier 6	0		Fixed	Fixed	The weaker smart rock was placed at the bottom of the river at 4 ft away from Pier 7 (east side).
		0		Fixed	Fixed	
		0		Fixed	Fixed	
		0	River flow	Fixed	Fixed	
6	On the downstream shoulder of bridge deck at Pier 7	0		Fixed	Fixed	
		0		Fixed	Fixed	
		0		Fixed	Fixed	
		0	River flow	Fixed	Fixed	
7	On the downstream shoulder of bridge deck at Pier 8	90		Fixed	Fixed	
		90		Fixed	Fixed	
		90		Fixed	Fixed	
		90	River flow	Fixed	Fixed	
		0		Fixed	Fixed	
		0		Fixed	Fixed	
		0		Fixed	Fixed	
		0	River flow	Fixed	Fixed	
8	On the downstream shoulder of bridge deck slowly moved between Pier 8 to Pier 6	90	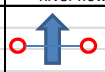	Pier 8 to Pier 6	Fixed	
		90		Pier 6 to Pier 8	Fixed	
		90		Pier 8 to Pier 6	Fixed	
		90	River flow	Pier 6 to Pier 8	Fixed	
		0		Pier 8 to Pier 6	Fixed	
		0		Pier 6 to Pier 8	Fixed	
		0		Pier 8 to Pier 6	Fixed	
		0	River flow	Pier 6 to Pier 8	Fixed	
9	On the downstream shoulder of bridge deck at Pier 8	90	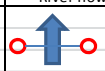	Fixed	N -> S	The weaker smart rock was placed at the bottom of the river at 4 ft away from Pier 7. The stronger smart rock was slowly moved along Pier 8 (west side).
		90		Fixed	S -> N	
		90		Fixed	N -> S	
		90	River flow	Fixed	S -> N	
		0		Fixed	N -> S	
		0		Fixed	S -> N	
		0		Fixed	N -> S	
		0	River flow	Fixed	S -> N	
10	On the downstream shoulder of bridge deck at Pier 7	90		Fixed	N -> S	
		90		Fixed	S -> N	
		90		Fixed	N -> S	
		90	River flow	Fixed	S -> N	
		0		Fixed	N -> S	
		0		Fixed	S -> N	
		0		Fixed	N -> S	
		0	River flow	Fixed	S -> N	
11	on the shoulder of bridge near downstream at Pier 6	90		Fixed	N -> S	
		90		Fixed	S -> N	
		90		Fixed	N -> S	
		90	River flow	Fixed	S -> N	
		0		Fixed	S -> N	
		0		Fixed	N -> S	
		0		Fixed	S -> N	
			River flow			
12	Underneath the bridge near Pier 8 (west side)	90		Fixed	N -> S	
		90		Fixed	S -> N	
		90		Fixed	N -> S	
		90	River flow	Fixed	S -> N	
		0		Fixed	N -> S	
		0		Fixed	S -> N	
		0		Fixed	N -> S	
		0	River flow	Fixed	S -> N	

Test Results and Discussion: Figs. 5-7 present a consolidated sample of data collected from the passive sensor testing at Roubidoux Creek. Figs. 5(a-c) represent the gradient change when the magnetometer remained stationary and the passive smart rock was moved along the same path between downstream (north or N) and upstream (south or S). Though the smart rock was moved along the same path each time, the distance from the magnetometer is different when the magnetometer was located in Pier 6 to Pier 8. As the magnetometer was relocated further from the sensor path, the angle spanned from the magnetometer to Point A (farthest upstream) and Point B (farthest downstream) decreased, which in turn reduced the change in distance experienced by the magnetometer and resulted in less change in magnetic gradient measurement from Pier 7 to Pier 6 or Pier 8.

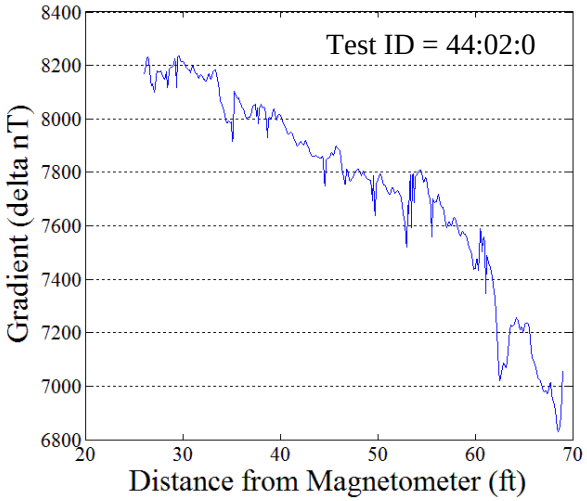

(a) Magnetometer stationed above Pier 7

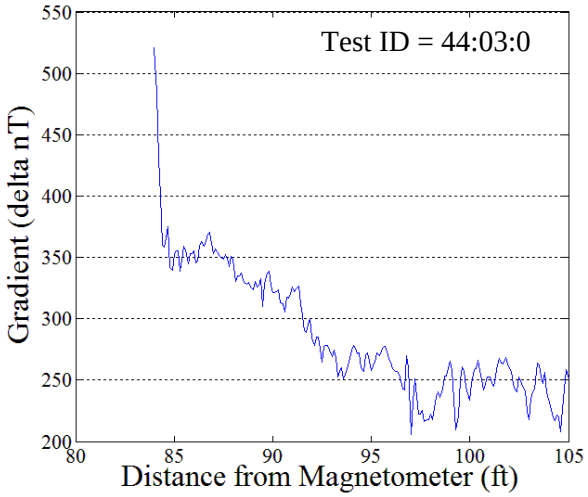

(b) Magnetometer stationed above Pier 8

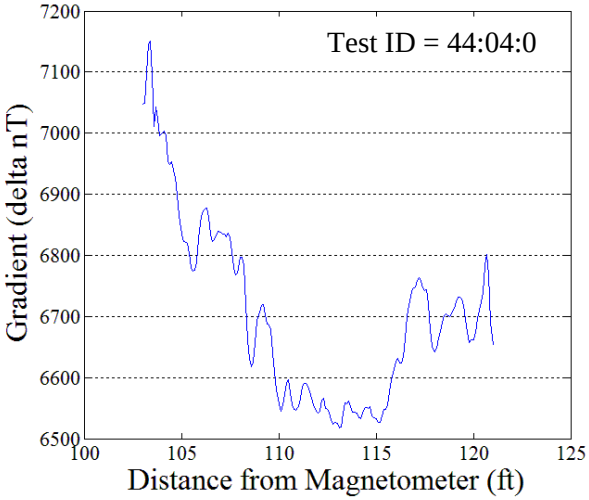

(c) Magnetometer stationed above Pier 6

Fig. 5 Magnetic gradient versus distance relations

Figs. 5(a-c) demonstrate a general decaying trend of the magnetic field intensity as the smart rock moves away from the magnetometer. The local fluctuations along this trend are likely due to the change in magnetic orientation as the smart rock was dragged and moved along the riverbed topography, which was clearly observed during the laboratory tests reported in the previous quaterly report.

Fig. 6 presents the magnetic field gradient as a function of distance as the magnetomter was moved away from Pier 6 to Pier 8 when the weaker smart rock was placed near Pier 7. Why a significant fluctuation exists in this case will be investigated in the next quarter. Note that the span length between Piers 6 and 7 is 80' while the span length between Piers 7 and 8 is 100'.

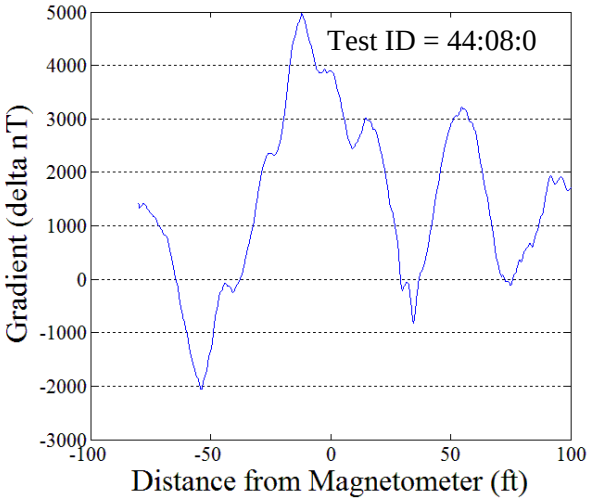

Fig. 6 Steady movement of the magnetometer away from the fixed smart rock at 4' from Pier 7

Figs. 7(a-d) confirm the same trend as indicated by Figs. 5(a-c). However, the field intensities in Figs. 7(a-d) seem to decrease with distance more rapidly than those in Figs. 5(a-c) since they were measured with two sensor heads of the magnetometer aligned perpendicular to the water flow direction. Additionally, these tests were performed with the weaker smart rock placed at the bottom of the river 4' away from Pier 7 and the stronger smart rock was moved along the river bank on the west side of Pier 8. The distance in Figs. 7(a-d) was measured from Pier 8 instead of Pier 7 in Figs. 5(a-c) and 6. Each individual test point given in Figs. 5-7 represents an average of four (except for Case 11 with three data points) runs of the same test with the same parameters. However, a few variables were not controlled during the test to replicate a practical application. For example, the orientation of the two sensor heads of the magnetometer as it is moved along the path cannot be percisely constant and may thus cause a slight change between different tests. By taking an average of four test runs, this change can be minimized.

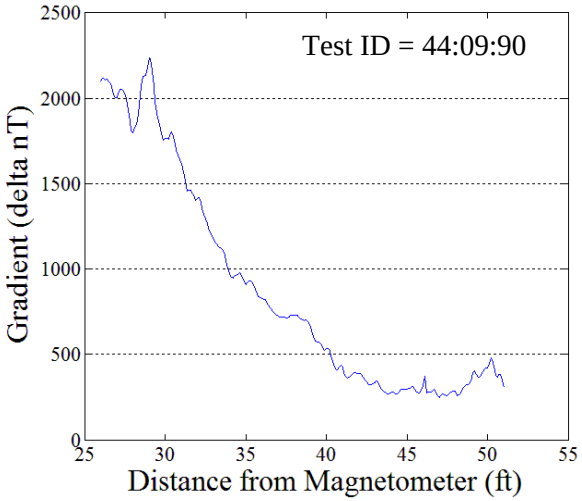

(a) Magnetometer stationed at Pier 8

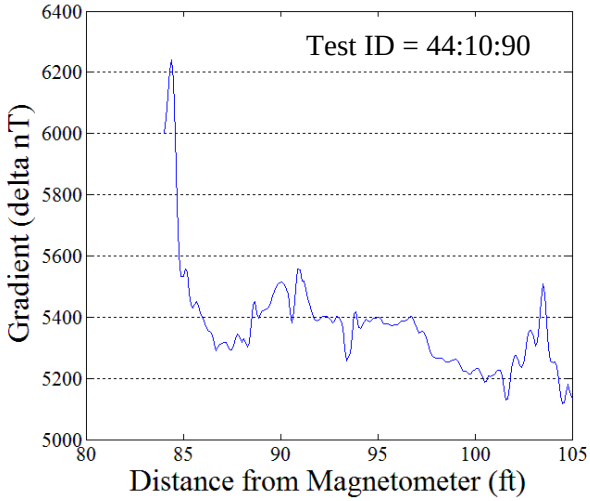

(b) Magnetometer stationed at Pier 7

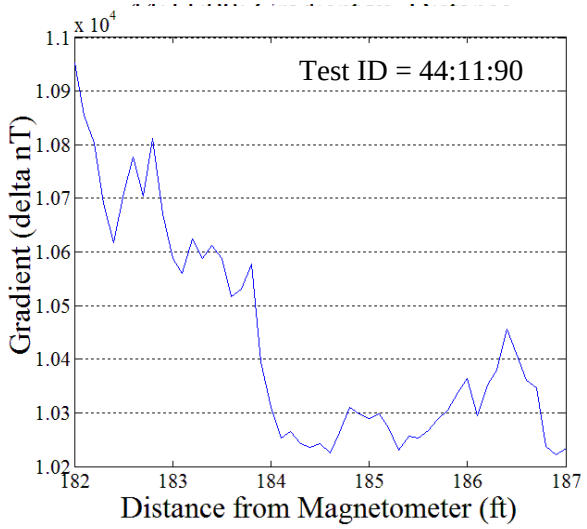

(c) Magnetometer stationed at Pier 6

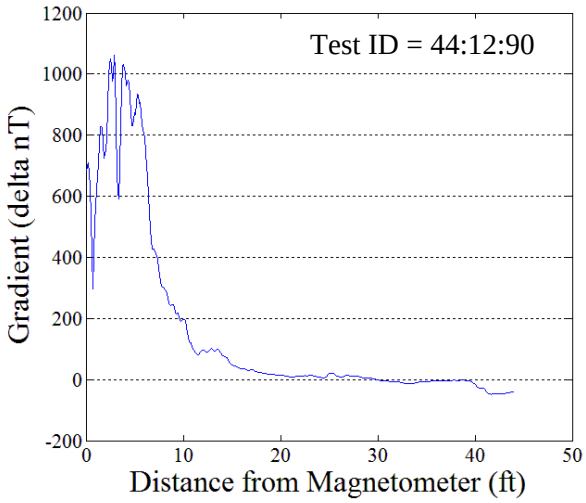

(d) Magnetometer stationed at Pier 8

Fig. 7 Magnetic field gradient versus measurement distance when the weaker smart rock was placed at 4" east of Pier 7 and the stronger smart rock was moved near Pier 8

Preliminary Conclusions with Passive Smart Rocks: The data acquired from this series of tests at Roubidoux Creek show promise in utilizing rare Earth magnets and a magnetometer as a passive sensing system for bridge scour monitoring as scour occurs. The overall decaying trend is consistent and repeatable as demonstrated with local fluctuations due to changing orientation of the neodymium magnet. Note that the results obtained from the two bridges are consistent.

Task 1.2 Steel Interferences to Magnetic Measurements – Noise Level, Data Cleansing and Engineering Interpretation with Passive Rocks Submitted

The previous report already indicated that the gradient measurement mainly removed the Earth's magnetic field. There is no clear sign of indication that the noise level in the gradient readings was reduced by the subtraction between the readings from two sensor heads of a magnetometer.

Task 2.1 Active Smart Rocks with Embedded Controllable Magnets or with Embedded Electronics – Engineering Design and Validation of Active Smart Rocks Submitted

Since we focused on the field tests at two bridge sites in the past quarter, no further work was done with embedded controllable magnets during the past quarter.

Task 2.2(a) Magneto-Inductive Communications – Engineering Design and Validation of Magneto-Inductive Transponders Submitted

In the past quarter, the active smart rocks tested in the hydraulic engineering laboratory at Turner-Fairbank Highway Research Center in June, 2012, were modified by mainly increasing the size of antenna. Two active smart rocks were deployed in the proximity of a bridge pier at each bridge site. Communication was attempted from the river bank and the bridge deck. Due to limited space, only the test results with the U.S. Highway 63 Gasconade River Bridge, Maries County, MO, are included in this report. Test was conducted on September 24, 2012.

Design and Casting of Active Smart Rocks with Magneto-Inductive Wireless Transmission
The Smart Rock v.2.4 electronic modules were used for the bridge tests. Compared to the laboratory tests in June 2012 included in the previous report, the following modifications for active smart rocks were made for field tests:

- A larger transmitting antenna (~9") was used for longer distance transmission,
- Transmitting and receiving parts of the electronic boards were re-tuned to the new antenna,
- Special high capacity / long term batteries were integrated into the boards, and
- Smart Rock boards were encased in concrete spherical blocks.

The printed circuit board with the on-board accelerometer module was oriented in parallel with the antenna plane. The Kaito AN-200 antennas (equivalent to the previously tested Grundig AN-200) were used for active smart rocks. They typically operate in a frequency range of 520 KHz-1510 KHz, which is off the 125 KHz frequency of an active smart rock communication link. To tune the antennas (345 μH in inductance) into the carrier frequency (125 KHz) in communication link, low-loss Mica capacitors of 4.7 nF were used. A perfectly-tuned antenna can operate most effectively in transmission/receiver stages but drain a current of more than 1.5 A, which is less desirable for long-term power management. To reduce current consumption during transmission, the transmission stage of the antenna connection circuit was slightly detuned from the ideal 125 KHz resonance to ensure that the maximum current level is less than 1 A.

Each active smart rock was powered by a pack of low self-discharge rate batteries – Tadiran TL5930/T, which can potentially last in charged/operational conditions for more than 10 years. Each battery can supply a pulse current up to 500 mA; but the performance datasheet recommended that a continuous current not exceed 230 mA. To assure a stable power supply for the active smart rock, a pack of four TL5930/T batteries was used for each smart rock module. Additionally, a super capacitor of 5 F was applied to the battery pack to improve dynamic response of the batteries. With a voltage of 3.6 V, the capacity of a single battery is 19 A-h.

For each active smart rock, the electronic boards, a transmitting antenna and batteries pack were enclosed into a watertight plastic bucket with an insulation gasket lid. To ensure waterproofing, the closure area between the bucket and the lid was heavily covered with waterproof silicone. The sealed bucket was then placed inside a thick concrete shell for protection. To prevent unexpected movement, the battery pack, electronic boards, and antenna were fixed by filling the interior of the waterproof bucket with construction foams as illustrated in Fig. 8.

Fig. 8 Smart rock v2.4 board and deployment near the scour-susceptible pier

To fit the large antenna and other small electronic parts placed inside the waterproof bucket, a 10” deep and 10”-diameter cylindrical cavity was designed inside a spherical concrete shell. With such a large cavity, an outer diameter of at least 16” must be used for the concrete sphere to ensure a sufficient specific gravity of over 2. Each concrete shell was cast with two halves of a 16”-diameter plastic sphere as illustrated in Figs. 9(a, b). The top half of the plastic sphere was cut to leave a 13”-diamter hole for insertion of the sealed bucket with electronics as shown in Fig. 9(b). The finishing open space of the concrete shell was covered by a cylindrical concrete cap as illustrated in Fig. 9(c).

(a) Bottom half of the mold (b) Top half of the mold and cavity (c) Concrete shell and cap

Fig. 9 Casting of concrete shells and caps

Improvements in Base Station / Link Control System The base station / link control system for smart rock operation has been packaged into professional enclosure units, making it more portable and easier to use. The analog demodulator circuitry was redesigned and PCB-manufactured. The required power supplies (+- 6 V, +- 15 V and +12 V) were integrated into the packaged enclosures. Fig. 10 shows photos of the two main units of a base station system: Base Station Receiver (left) and Wake Up Signal Transmitter Controller/Amplifier (right).

Fig. 10 Two main modules of the Analog Base Station

Fig. 11 shows a schematic of the redesigned Analog Demodulator module. The PCB-based module is more controllable and mechanically stable. The new design is based on Analog Devices 8032 single supply voltage feedback amplifiers and provides outputs for easy tuning of demodulation threshold settings.

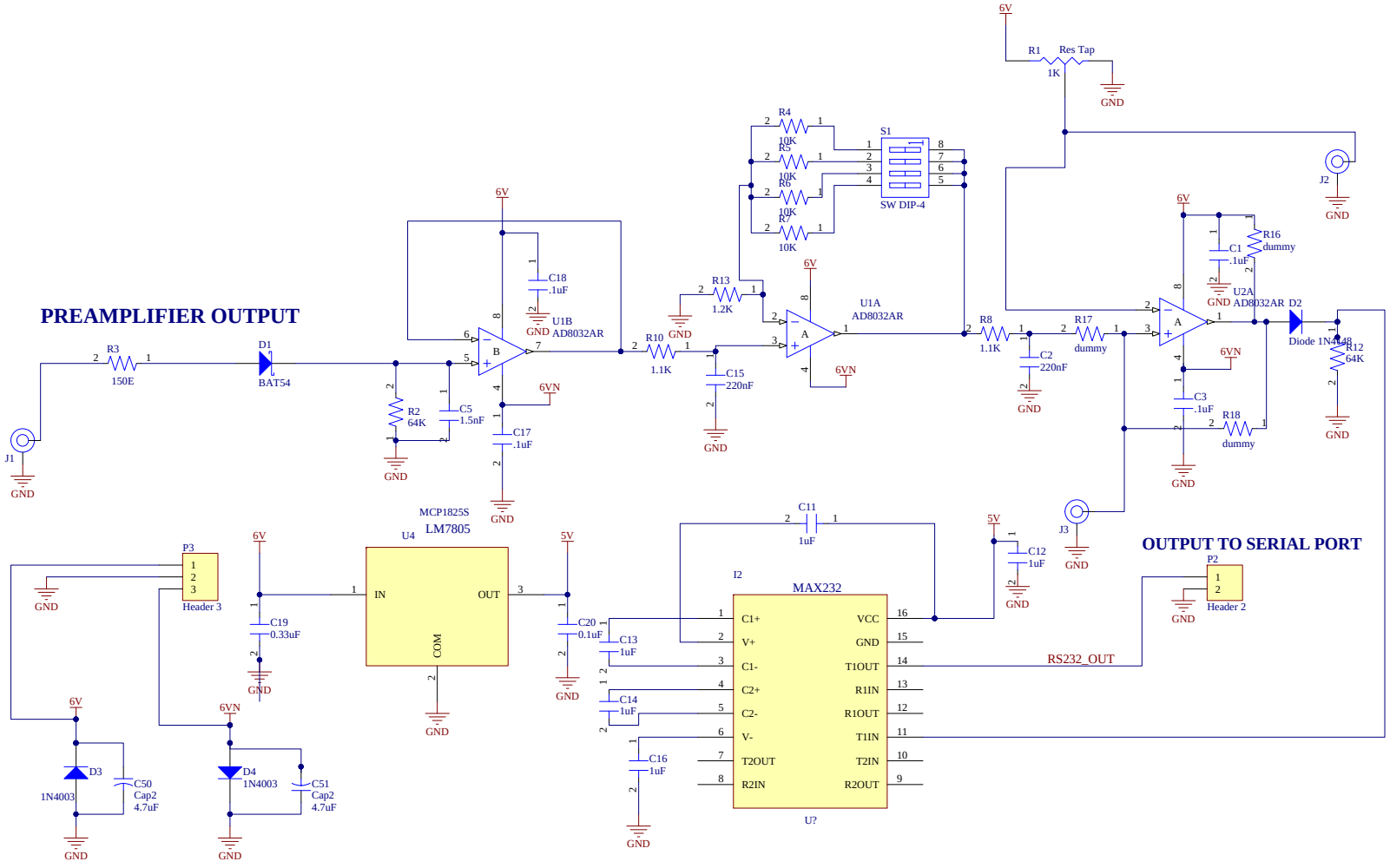

Fig. 11 A schematic of the redesigned demodulator

Figs. 12 and 13 show a modular structure of the Analog Base Station Unit and a demodulator board with input/output connections. The Analog Base Station Unit includes:

- EMI filter socket for power line conductive emissions reduction
- +- 6 V linear power supply
- 4 125 KHz band-pass filters / preamplifiers for antennas connection
- 4 port log detector
- Demodulator with an RS232 output interface

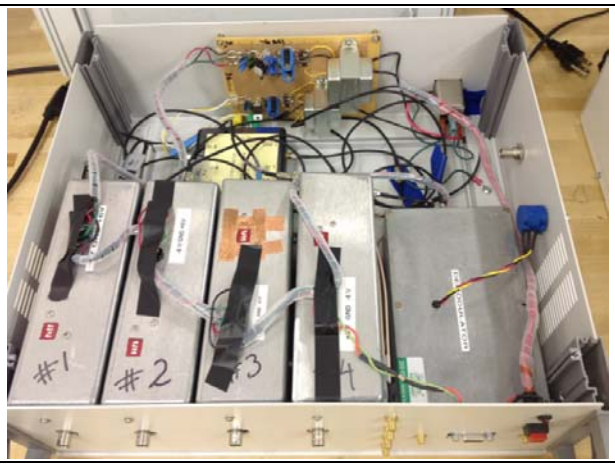

Fig. 12 Modular structure of the Analog Base Station Unit

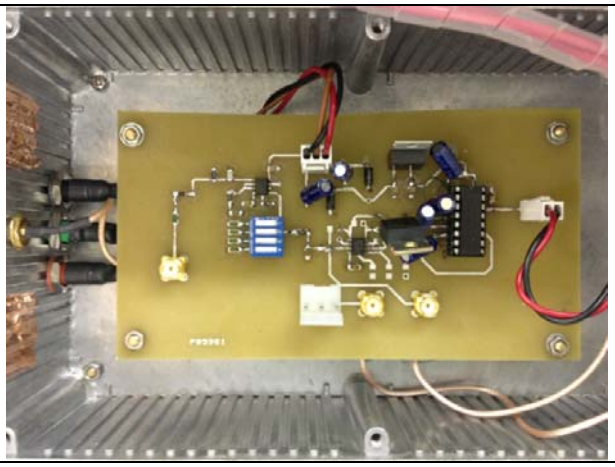

Fig. 13 Demodulator board with input/output connections

Bridge Tests and Results

Fig. 14 shows the antennas placement when communicated from the bridge deck and the base stations at two locations: river bank and bridge deck. The bridge deck was approximately 55'-58' above the water; the distance from the bridge deck station to the active smart rocks placed under water was about 65'.

(a) Four antenna holders

(b) Base station at river bank

(c) Base station at bridge deck

Fig. 14 Test setup at the Gasconade River Bridge on the U.S. Highway 63

During communication tests, two smart rocks (designated as A and B) were separately waken up and transmitted data. Fig. 15 shows the data signal patterns received from the two rocks in response to the wake-up signal transmission when the gain of preamplifiers was set to 500.

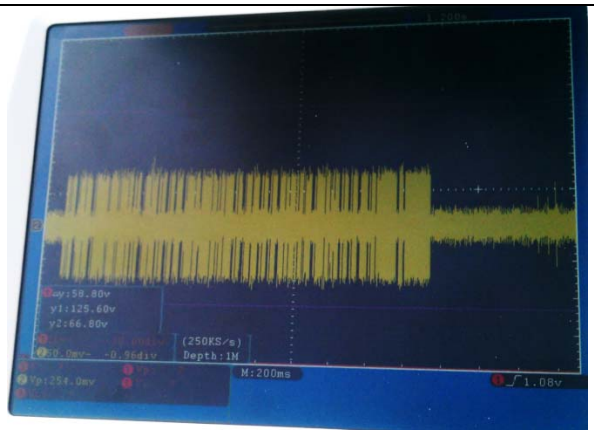

(a) Rock A

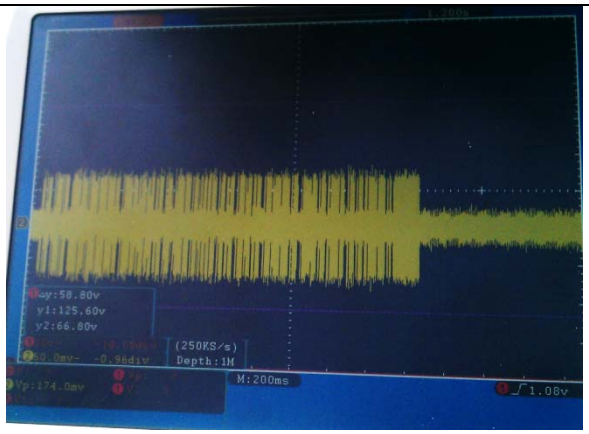

(b) Rock B

Fig. 15 Signal responses from the two smart rocks

It can be observed from Fig. 15 that the peak-peak noise and signal levels are approximately 50 mV and 150 mV, respectively. These results demonstrated a robust operation of wake-up interface via electromagnetic radiation responses from the underwater smart rock. The maximum communication distance depends on the relative orientation between the smart rock antenna and the receiving antenna bundles. It exceeded 30' from the river bank and 60' from the bridge deck.

During the bridge tests, initial pitch and roll parameters of the smart rocks placed under water were recorded. However, localization of the smart rocks was not yet performed since calibration tests with a heavy active smart rock (approximately 150 lbs each) at the bridge site are impractical. Analytical or simulation-based calibration / localization methods are currently under way.

The field testing also validated the waterproof casing of smart rock electronic components. In particular, repeated tests were conducted to ensure no change in the orientation of the accelerometers and magnetometers embedded in the smart rock, which could occur with significant water leakage. Additionally, the batteries pack continued to supply the required power throughout the testing.

Task 2.2(b) Acoustic Communications – Engineering Evaluation of Acoustic Communication Systems for Bridge Scour Monitoring

In this quarter, an acoustic communication system has been developed and tested using the Texas Instrument Digital Signal Processor TMS320C6713. As illustrated in Fig. 16, the transmitter consists of a 'C6713 board, a digital-to-analog converter (DAC), a power amplifier, and an acoustic projector. The receiver consists of two channels of hydrophones, LNA (low-noise amplifier), and ADC (analog-to-digital converter), interfacing with one 'C6713 board.

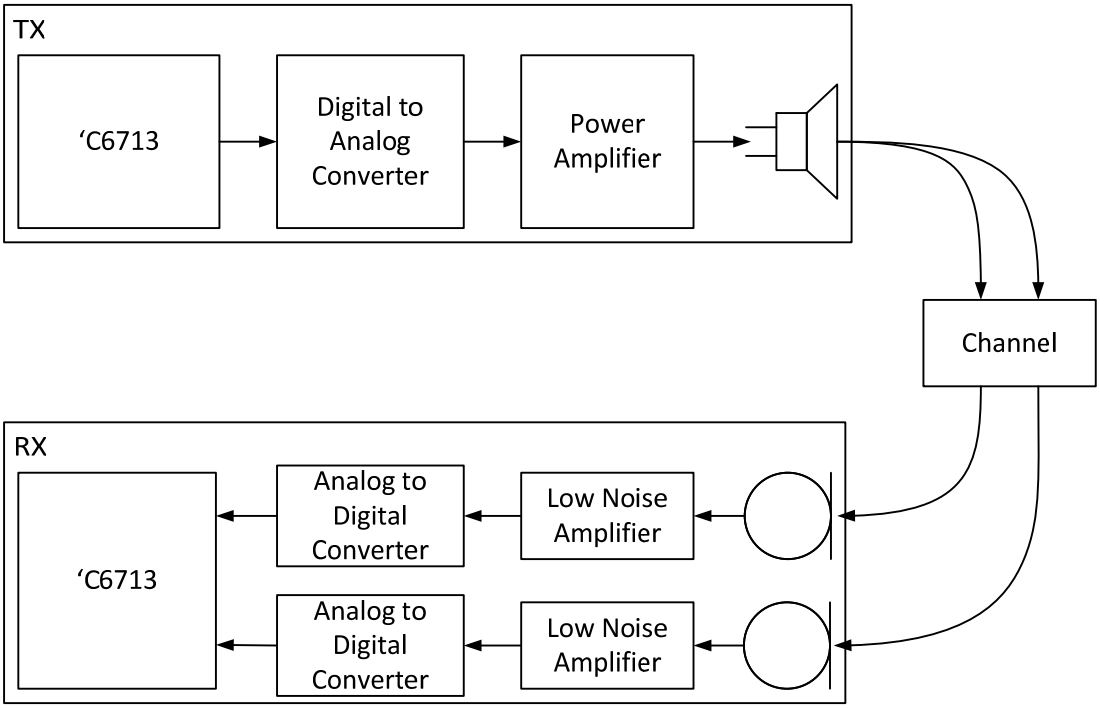

Fig. 16 Acoustic communication system

The acoustic communication system was tested at the two bridge sites. The base communication station was deployed at the river bank and an acoustic projector and hydrophones were submerged in water. The test results and experiences are briefly reported below.

At the U.S. Highway 63 Gasconade River Bridge, the signals received by the base station were observed on the oscilloscope and the DSP platform. At a distance of approximately 50', the received signals were 100 mV (peak-peak) using the pre-amplified hydrophone. The signals appeared to be very clean with the estimated SNR above 10 dB. However, raw data was not saved during the field tests; the detection algorithm with the DSP C++ programming was problematic, resulting in an error rate of over 20%. It was found that the power failure of power supply boxes occurred likely due to improper grounding of the power supply when connected to the power generator. The DSP boards were later powered by external power supplies that have protection circuits.

At the Interstate 44 Roubidoux River Bridge, the acoustic projector and hydrophones were submerged in the shallow river with an estimated water depth of 5'. Two measurement distances were tested: 3' and 15'. The test results at the 3' distance are presented in Fig. 17. The received raw data appeared clean with no short burst prior to each block. The 79-bit blocks were properly separated by gaps of zeros as well. At this bridge site, the Channel 1 reading was weak and Channel 2 reading was strong. However, the SNRs were around 8.5 dB, similar to those for the Gasconade River Bridge. The detected bits for the first block show 4-bit error and no error for Channels 1 and 2, respectively. Overall, the bit error rate was about 2%.

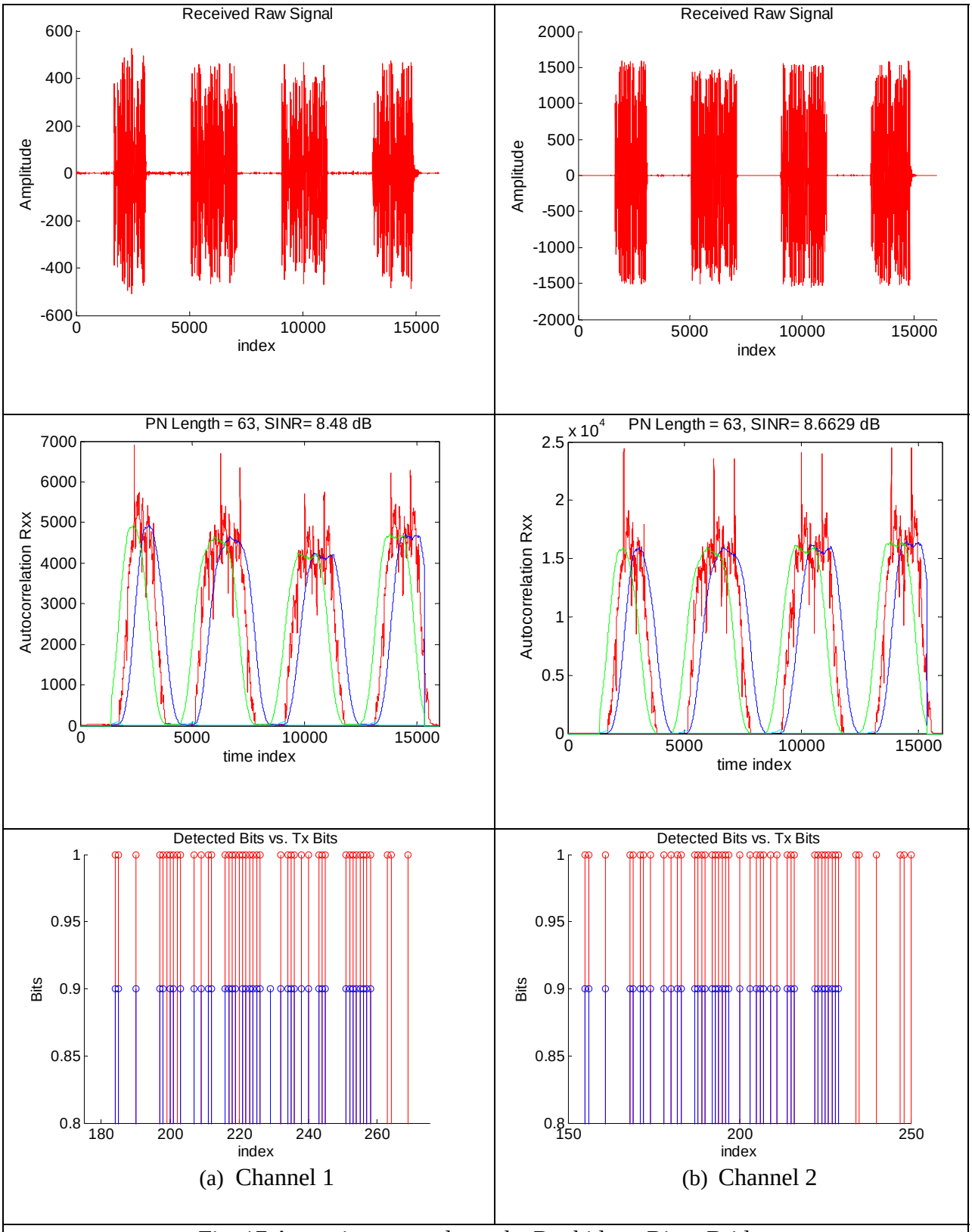

(a) Channel 1

(b) Channel 2

Fig. 17 Acoustic test results at the Roubidoux River Bridge

Task 3.2 Field Validation Planning and Execution – Field Test Plan and Data Analysis Submitted

As presented in the previous sections, both passive and active smart rocks were tested at two bridge sites.

I.2 PROBLEMS ENCOUNTERED

There are no problems encountered in this quarter. However, the project continued to be delayed for about three months as explained in the previous report. On the other hand, the project expenditure is in general agreement with the project progress.

I.3 FUTURE PLANS

Three subtasks will be executed during the next quarter. A brief description of various activities in each subtask is described below:

Task 1.1 Design, fabricate, and test in laboratory and field conditions DC magnetic sensors with embedded magnets aligned with the earth gravity field. Summarize and document the test results and the performance of passive smart sensors.

More laboratory characterizations will be conducted with large magnets that were used in the bridge tests. With the new calibration test results, the field test data can be applied to localize the passive smart rock placed in the river near Pier 7. Additionally, an attempt will be made to build small smart rocks with an automatic alignment function of the embedded magnet and thus enhance the smart rock sensitivity.

Task 1.2 Research, summarize, and document the degree of potential steel interferences to magnetic measurements. Investigate ways to compensate the interference effect and develop a rock localization technique.

Further tests will be conducted in laboratory to characterize how adjacent metals affect the magnetic field measurement.

Task 2.1 Design, fabricate, and test in laboratory and field conditions active smart rocks with embedded controllable magnets or with embedded electronics. Summarize and document the test results and the performance of active smart rocks.

Active smart rocks with controllable magnets will be designed, fabricated, and tested.

Task 2.2(a) Design, fabricate, and test in laboratory and field conditions magneto-inductive transponders. Summarize and document the test results and the performance of transponders.

The new design of Smart Rock Electronic Board (v.3) will be built in the third week of October, 2012. It will include:

- Upgraded PIC16LF1829 microcontroller
- On-board memory module
- Current-driven solution for antenna excitation
- Improvements and fixes

One of the most important features is the arrangement of communication within the network of smart rocks to enable the estimate of relative Received Signal Strength Indications (RSSI) of all rocks in the network. Production of 12 electronic boards is currently planned, allowing the testing of more configurations of a distributed smart rock network structure.

To simplify the smart rock production process, the antenna can be printed on PCB together with the board layout itself. A prototype of such an antenna was already made and will be tested in the next quarter. When Smart Rock v.3 units are ready for implementation, the previously deployed smart rocks will be extracted from the river and replaced by the new units.

For easy replication of field tests, integration of a smart rock base station in a mobile vehicle will be considered. In this way, only receiving/wake up transmitting antennas need to be deployed upon arrival at a bridge site and the time to set up the base station for field tests can be greatly reduced.

Task 2.2(b) Research, summarize, and document current underwater acoustic transmission practices and required modifications for bridge scour monitoring.

The C++ codes will be further verified for robust performance in laboratory and field tests. In addition, more robust hardware in professional packaging will be built.

Task 3.2 Plan and execute the field validation tasks of various prototypes. Analyze the field performance of smart rocks and communication systems.

Initial field tests at two bridge sites were completed. The field test data will continue to be processed for the evaluation of field performance of various technologies.

II – BUSINESS STATUS

II.1 HOURS/EFFORT EXPENDED

The planned hours and the actual hours spent on this project are given and compared in Table 2. In the fifth quarter, the actual hours are literally the same as the planned hours. However, the actual cumulative hours are approximately 50% of the planned hours, corresponding to the project delay starting the third quarter. The cumulative hours spent on various tasks by personnel are presented in Fig. 18.

Table 2 Hours spent on this project

	Planned		Actual	
	Labor Hours	Cumulative	Labor Hours	Cumulative
Quarter 1	752	752	184	184
Quarter 2	752	1504	345	529
Quarter 3	752	2256	381	909
Quarter 4	752	3009	166	1075
Quarter 5	720	3729	721	1877

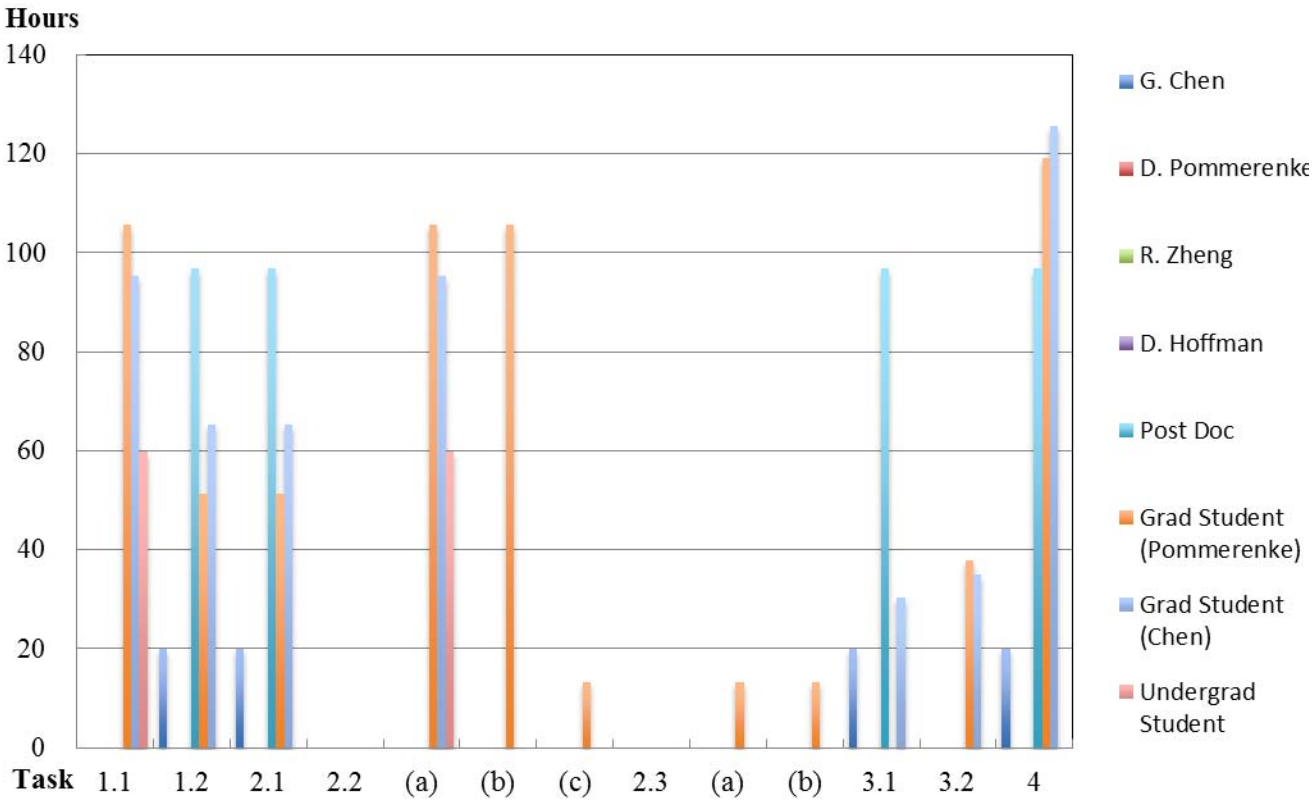

Fig. 18 Cummulative hours spent on various tasks by personnel

II.2 FUNDS EXPENDED AND COST SHARE

The budgeted and expended RITA funds accumulated by quarter are compared in Fig. 19. Approximately 46% of the budget has been spent till the end of fifth quarter. During the fifth quarter, 58% of the budget has been spent. The actual cumulative expenditures from RITA and Missouri S&T/MoDOT are compared in Fig. 20. The expenditure from RITA is significantly less than the combined amount from the Missouri S&T and MoDOT.

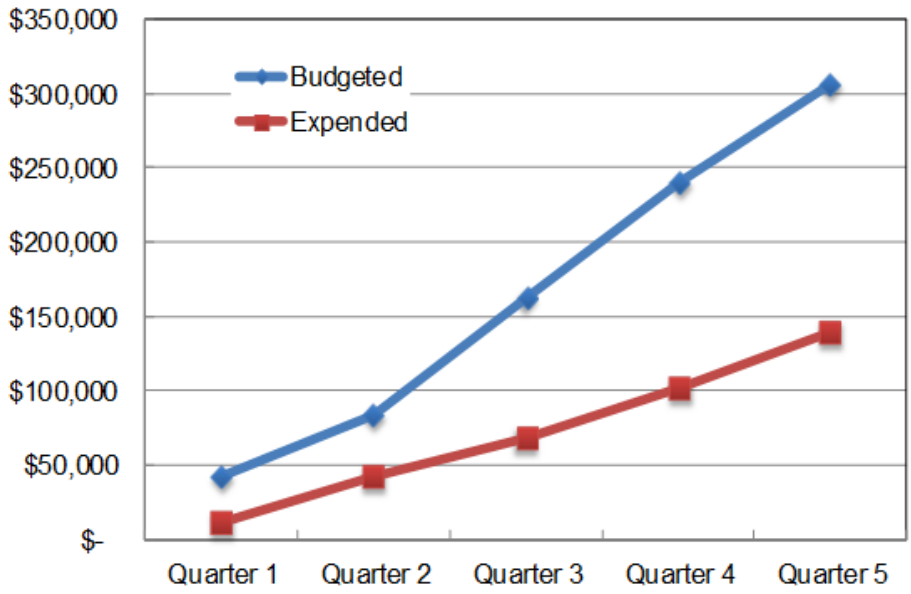

Fig. 19 Comparison of RITA budget and expenditure accumulated by quarter

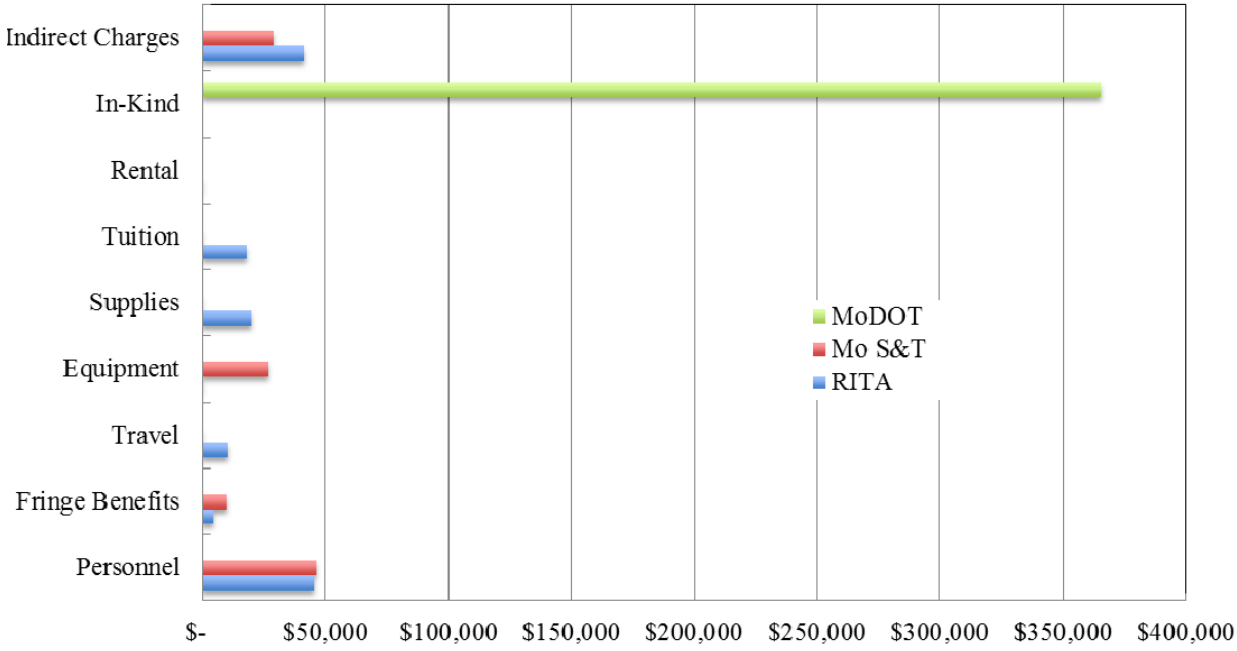

Fig. 20 Cummulative expenditures by sponsor